Comparison of Geometric and Probabilistic Shaping with Application to ATSC 3.0

Fabian Steiner*, Georg Böcherer†
*Fachgebiet Methoden der Signalverarbeitung
†Institute for Communications Engineering
Technical University of Munich
Email: {fabian.steiner, georg.boecherer}@tum.de

Abstract—In this work, geometric shaping (GS) and probabilistic shaping (PS) for the AWGN channel is reviewed. Both approaches are investigated in terms of symbol-metric decoding (SMD) and bit-metric decoding (BMD). For GS, an optimization algorithm based on differential evolution is formulated. Achievable rate analysis reveals that GS suffers from a 0.4 dB performance degradation compared to PS when BMD is used. Forward-error correction simulations of the ATSC 3.0 modulation and coding formats (modcods) confirm the theoretical findings. In particular, PS enables seamless rate adaptation with one single modcod and it outperforms ATSC 3.0 GS modcods by more than 0.5 dB for spectral efficiencies larger than 3.2 bits per channel use.

I. INTRODUCTION

Bandwidth-efficient communication requires to use higher-order modulation formats, such as M-amplitude shift keying (ASK), M-quadrature amplitude modulation (QAM) or M-amplitude phase-shift keying (APSK) constellations. On the additive white Gaussian noise (AWGN) channel model, discrete, equidistant constellations with uniform signaling result in a gap to capacity of 1.53 dB in the high signal-to-noise-ratio (SNR) regime [1, Sec. IV-B].

In order to compensate for this performance loss, probabilistic shaping (PS) and geometric shaping (GS) can be employed in order to mimic a "Gaussian-like" shape of the constellation. PS imposes a non-uniform distribution on a set of equidistant constellation points. We refer to [2, Sect. II] for a literature review on probabilistic shaping approaches. As the desired distribution needs to be ensured at the channel input, some schemes perform the shaping operation *after* forward error correction (FEC) encoding and it is reversed before decoding. This is prone to error propagation and usually requires iterative processing at the receiver [3]. In [2], probabilistic amplitude shaping (PAS) is introduced which concatenates encoding and shaping in reverse and enables a simple receiver setup.

Geometric shaping employs a uniform distribution on non-equidistant constellation points. The authors of [4] show that this approach achieves the capacity of the AWGN channel

if the number of constellation points goes to infinity. In [5], the effect of geometric shaping is investigated in terms of the achievable rate when both symbol-metric decoding (SMD) and bit-metric decoding (BMD) are employed on one-dimensional constellations. The numerical results indicate that both optimization criteria lead to different optimized constellations. Recently, geometrically shaped constellations were included in the DVB-NGH [6], [7] and ATSC 3.0 standards [8], [9], where they are generally referred to as non-uniform constellations (NUCs).

The contributions of the present work are twofold.

- We provide a comprehensive comparison of both PS and GS in terms of their information theoretic achievable rates for SMD and BMD. To this end, we propose a differential evolution (DE) [10] based optimization approach to obtain optimized geometrically shaped constellations. The results show that GS has a gap to capacity of about 0.4 dB, when BMD is used. In contrast, PS with BMD virtually achieves capacity.

- We compare a selection of ATSC 3.0 modcods, i.e., modulation order and code rate combinations, to a PS system operating with a single modcod using PAS [2]. FEC simulations show that the information theoretic gains translate into practical, coded performance improvements to a full extent.

The work is organized as follows. In Sec. II, we present the system model. Sec. III states the optimization procedures for both GS and PS. We present FEC simulation results in Sec. IV and conclude in Sec. V.

II. SYSTEM MODEL

We consider the discrete time AWGN channel

$$Y_i = X_i + Z_i, \quad i = 1, \ldots, n_\mathrm{c} \tag{1}$$

for a transmission block of n_c channel uses. The time indices are omitted in the following. As we consider both one and two dimensional constellations, the noise Z is either zero mean Gaussian, or zero-mean, circular symmetric complex Gaussian. Accordingly, the channel input X originates from an M-ary real or complex signaling set $\mathcal{X}$. We define SNR $= \mathrm{E}\left[|X|^2\right] / \mathrm{E}\left[|Z|^2\right]$. The random variables X and Z are either

both real or both complex; the resulting SNR is the same in both cases. For each dimension, the capacity is given by

$$\mathsf{C}(\mathrm{SNR}) = \frac{1}{2}\log_2(1 + \mathrm{SNR}). \qquad (2)$$

For practical systems, a Gaussian codebook is not feasible so that discrete constellations like ASK and QAM are employed. To combine $M = 2^m$-ary higher-order constellations with FEC, a code over $\mathrm{GF}(M)$ can be used and the field elements are directly mapped to constellation points. However, this usually comes at the price of increased decoding complexity [11, Sec. IV]. At the receiver, different decoding metrics can be employed. For non-binary FEC, one typically uses SMD with the decoding metric $q(x, y) = p_{Y|X}(y|x)P_X(x)$ and an achievable rate is given by the mutual information $\mathrm{I}(X;Y)$, i.e.,

$$\mathsf{R}_{\mathrm{SMD}}(P_X, \mathrm{SNR}) = \mathrm{I}(X;Y). \qquad (3)$$

To use a binary FEC, a binary labeling of the signal points has to be introduced. Hence, each signal point $x_{\boldsymbol{b}} \in \mathcal{X}$ is assigned a binary m-bit label of the form $\boldsymbol{b} = b_1 b_2 \ldots b_m$ with $b_i \in \{0, 1\}, i = 1, \ldots, m$. In this case, usually a *pragmatic* approach with a bitwise-metric is pursued, consisting of a binary soft demapper followed by a binary decoder. This approach was introduced in [12] and is now often called bit-interleaved coded modulation (BICM) [13]. It can be motivated by a mismatched decoding perspective [14], where the decoding metric $q(x, y) = q(x_{\boldsymbol{b}}, y) = \prod_{i=1}^{m} p_{y|B_i}(y|b_i)P_{B_i}(b_i)$ is used to arrive at the information theoretic model of m parallel channels with

$$p_{Y|B_i}(y|b) = \frac{1}{P_{B_i}(b)} \sum_{\xi \in \mathcal{X}_i^b} p_{Y|X}(y|\xi)P_X(\xi).$$

Here, the set $\mathcal{X}_i^b \subseteq \mathcal{X}$ refers to all constellation points which have the i-th bit in their binary label set to b. In [15], it was recently shown that an achievable rate is given by

$$\mathsf{R}_{\mathrm{BMD}}(P_X, \mathrm{SNR}) = \left[\mathrm{H}(\boldsymbol{B}) - \sum_{i=1}^{m} \mathrm{H}(B_i|Y_i) \right]^+. \qquad (4)$$

Remark 1. In case of uniform inputs, the BMD achievable rate (4) can be rewritten as $\mathsf{R}_{\mathrm{BMD}} = \sum_{i=1}^{m} \mathrm{I}(B_i; Y)$, which is commonly known as *BICM capacity* [14].

We will also employ the notation $\mathsf{R}_{\mathrm{BMD}}^{-1}(P_X, R)$ to denote the required SNR to achieve a BMD rate R, i.e., $\mathsf{R}_{\mathrm{BMD}}(P_X, \mathrm{SNR}) = R$. If P_X is omitted, a uniform distribution on the constellation points is assumed in both cases.

Using the chain rule of mutual information, it can be shown that $\mathsf{R}_{\mathrm{BMD}} \leq \mathsf{R}_{\mathrm{SMD}}$ and clearly, $\mathsf{R}_{\mathrm{SMD}} \leq \mathsf{C}$. The rate $\mathsf{R}_{\mathrm{BMD}}$ depends on the employed labeling and a binary reflected Gray code (BRGC) [16] usually performs well.

III. GEOMETRIC AND PROBABILISTIC SHAPING

A. Geometric Shaping

Geometric constellation shaping employs non-equidistant spacing of the constellation points with a uniform distribution.

Algorithm 1 Summary of the DE algorithm to find the best constellation for a given SNR.

INPUT: SNR, constellation size M, candidate set size P, number of generations G, crossover probability p_c, amplification factor F.
1: Create feasible initial population set $\{\tilde{\mathcal{X}}_p\}_{p=1}^{P}$ at random.
2: Evaluate metric $\mathsf{R}_{\{\mathrm{BMD,SMD}\}}$ for each population member.
3: **for** $g = 1, \ldots, G$ **do**
4:      **for** $p = 1, \ldots, P$ **do**
5:          Choose $r_1 \neq r_2 \neq r_3$ randomly from $\{1, \ldots, P\}$.
6:          $\boldsymbol{T} = \mathtt{map}(\tilde{\mathcal{X}}_{r_1}^{(g-1)} + F \cdot (\tilde{\mathcal{X}}_{r_2}^{(g-1)} - \tilde{\mathcal{X}}_{r_3}^{(g-1)}))$
7:          $\boldsymbol{T} = \mathtt{mutate}(\boldsymbol{T}, \tilde{\mathcal{X}}_p^{(g-1)}, p_c)$
8:          Evaluate metric of new candidate $\boldsymbol{T}$.
9:          Set $\tilde{\mathcal{X}}_p^{(g)} = \boldsymbol{T}$, if metric has improved.
10:      **end for**
11:      **if** all population members have the same metric **then**
12:          Stop.
13:      **end if**
14: **end for**

The best constellation depends on the SNR and the employed metric. To facilitate the solution approach in the following, we refine (1) w.l.o.g. and impose $\mathrm{E}\left[|X|^2\right] \leq 1$ such that the SNR is given by $1/\mathrm{E}\left[|Z|^2\right]$. The optimization problem to find the optimized constellation $\mathcal{X}^*$ can be formulated as

$$\mathcal{X}^* = \underset{\substack{\mathcal{X}:\mathrm{E}\left[|X|^2\right] \leq 1 \\ |\mathcal{X}|=M}}{\mathrm{argmax}} \; \mathsf{R}_{\{\mathrm{BMD,SMD}\}}(\mathrm{SNR}). \qquad (5)$$

For both metrics, the optimization in $\mathcal{X}$ is non-convex. The works [5], [17] employed "constrained non-linear optimization algorithms" without providing more details on the actually employed optimization procedure. In [18], simulated annealing is used to optimize APSK constellations. Initial investigations by using standard, black box interior point algorithms like Matlab's fmincon showed that the obtained optimization results depend on the initialization, which suggests that only locally optimal solutions are found.

In the following, we propose an optimization based on differential evolution [10], which is a genetic algorithm and appears to find the global optimum, i.e., DE recovered previously reported results from arbitrary valid starting points.

DE starts with an initial population $\{\tilde{\mathcal{X}}_p\}_{p=1}^{P}$ of candidate constellations (see line 1). In each generation, a population member experiences a mutation. For this, DE randomly selects three distinct population members and combines them as shown in line 6. As the result of this operation may violate the feasible set, the function $\mathtt{map}(\cdot)$ implements a bounce back strategy. Eventually, the new candidate constellation is generated by replacing each component of $\tilde{\mathcal{X}}_p^{(g-1)}$ with probability p_c by the corresponding entry of $\boldsymbol{T}$. If the metric for the new candidate $\boldsymbol{T}$ has improved we keep it, otherwise we set $\tilde{\mathcal{X}}_p^{(g)} = \tilde{\mathcal{X}}_p^{(g-1)}$. We stop after G generations or once all population members have the same objective function value.

We distinguish between one-dimensional GS (1D-GS) and two-dimensional GS (2D-GS) and exploit symmetry to decrease the number of optimization parameters.

For 1D-GS and an M-ary 1D constellation (1D-GS 1D-NUC), each of the $M/2$ components of $\tilde{\mathcal{X}}_p$ is constrained to the non-negative real axis and the augmented, final constellation $\mathcal{X}_p$ with the negative part must fulfill the power constraint. A two-dimensional 1D-GS M-ary constellation (1D-GS 2D-NUC) can be obtained by the Cartesian product of two copies of 1D-GS $\sqrt{M}$-ary 1D-NUCs.

For 2D-GS, the population members are restricted to the first quadrant of the complex plane and $(M/4)\cdot 2$ real variables have to be optimized ($M/4$ for the real and $M/4$ for the imaginary part). This introduces additional degree of freedoms (DOFs) and leads to larger achievable rates.

To remain in the feasible set, i.e., on the real non-negative axis for 1D-GS and the first quadrant for 2D-GS, the `map` function (see line 6) replaces any negative real or imaginary part by its absolute value and rescales it to meet the power constraint.

In our trials, we used an amplification factor $F = 0.5$ and a crossover probability $p_c = 0.88$. The number of generations is set to $G = 10\,000$ and the population size was chosen depending on the number of DOFs as $P = 5\cdot\text{DOF}$. Choosing this parameter thoroughly turned out to be crucial in our experiments: Setting it too small, the optimum may not be found and setting it too large, the number of generations would not suffice. In the low and medium SNR regime, usually 100 to 1000 generations are enough to observe convergence.

If the metric targets BMD rates, the influence of the labels has to be taken into account as well. For 1D-GS, we randomly assign each component of $\tilde{\mathcal{X}}_p$ a $\log_2(M) - 1$ bit label. The labels for the augmented constellation $\mathcal{X}_p$ are then obtained by first replicating and then prefixing each half with a zero and one, respectively. For 2D-GS, the same approach applies, however, each quadrant in the augmented constellation is prefixed by one of the four two-bit labels 00, 10, 11 and 01 in an ordered manner, which is consistent with ATSC 3.0.

B. Probabilistic Shaping

In contrast to GS, PS uses a non-uniform distribution over equidistant constellation points. Contrary to the GS case, we instantiate (1) for the real case, i.e., w.l.o.g. $Z \sim \mathcal{N}(0,1)$ and set $X = \Delta\tilde{X}$, where the positive, real valued parameter denotes the spacing between the constellation points and $\tilde{X} \in \{\pm 1, \pm 3, \ldots, \pm 2^{m-1}\}$. The corresponding optimization problem reads as

$$P_X^* = \underset{P_X, \Delta > 0 : \mathbb{E}\left[\left|\Delta\tilde{X}\right|^2\right] \leq \text{SNR}}{\text{argmax}} R_{\{\text{SMD},\text{BMD}\}}(P_X, \text{SNR}). \quad (6)$$

For fixed Δ, R_{SMD} is convex in P_X [19, Ch. 4.4] and the following nested approach can be taken:

1) Parameter Δ is optimized using a simple line search.
2) For each fixed Δ during the line search, perform the optimization in P_X, using efficient and globally optimal

optimization algorithms like Blahut-Arimoto [20] or Cutting-Plane based approaches [21].

For BMD, the sequential approach can still be used, but R_{BMD} is not convex in P_X anymore.

This problem can be circumvented by optimizing over the Maxwell-Boltzmann (MB) distribution family [22]. As the numerical evaluations in Sec. III-C show, even this suboptimal approach virtually achieves capacity and outperforms the GS results, which are conjectured to be globally optimal. A detailed comparison of the optimal and MB based performance for both SMD and BMD is provided in [2, Table I, III].

Two-dimensional PS is obtained by taking two copies of the one-dimensional PS constellations.

C. Achievable Rates Comparisons

In the following, we compare the BMD and SMD achievable rates for both geometrically and probabilistically shaped constellations. As a performance metric we resort to the SNR gap to capacity. It is defined as

$$\Delta\text{SNR} = \text{SNR} - \mathsf{C}^{-1}(\mathsf{R}_{\text{BMD}}(P_X^*, \text{SNR})), \quad (7)$$

where $\mathsf{C}^{-1}(\cdot)$ represents the inverse capacity functional of the real or complex AWGN channel, respectively. P_X^* is either the uniform distribution $1/|\mathcal{X}^*|$ on $\mathcal{X}^*$ of (5) for GS or the optimal distribution for PS as the solution of (6). The obtained constellations are available from [23].
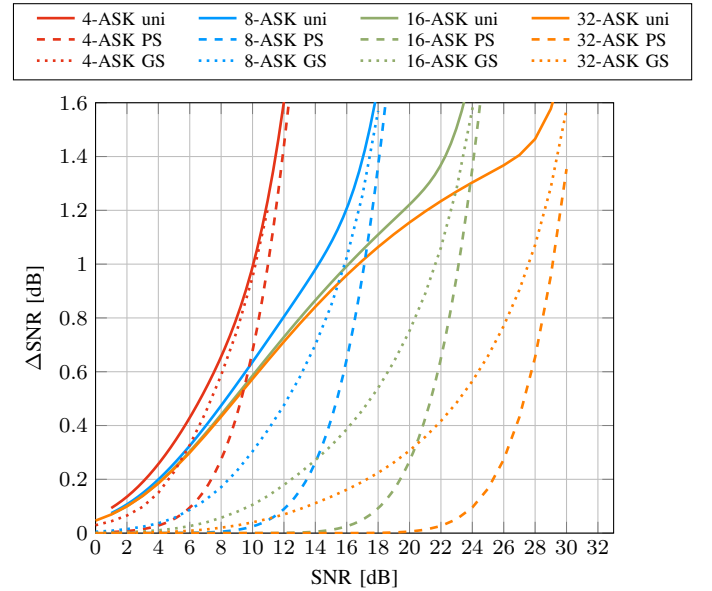

Fig. 1. SMD gap to capacity in dB for 1D-GS and PS.

Fig. 1 illustrates the gap to capacity for the optimized one-dimensional $\{4, 8, 16, 32\}$-ASK constellations in case of SMD. As a reference, we also plot the gaps for uniform, equidistant constellations. As derived in previous work [4], the shaping gain of geometrically shaped constellations increases with the constellation size.

Fig. 2 provides the equivalent evaluation for BMD. Here, the gap to capacity does not exhibit a monotonous behavior
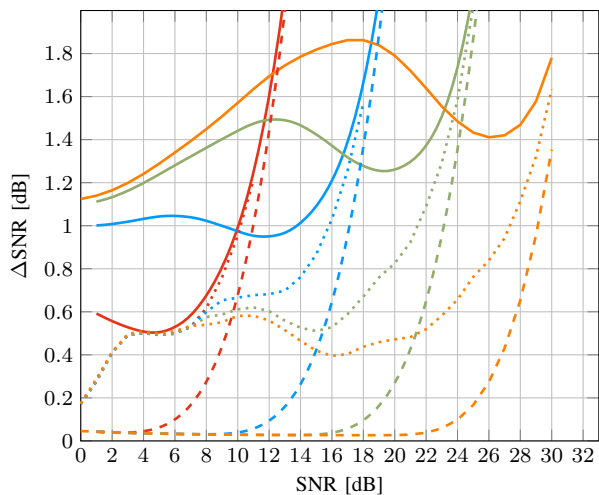
Fig. 2. BMD gap to capacity in dB for 1D-GS and PS.

and is particularly larger in the low to medium SNR regime, as there is an additional BMD penalty. PS shows improved performance over the whole range of constellations and SNR values. In particular, we observe that the gap to capacity remains almost constant in the order of 10^{-2} dB (with an improvement of more than 0.4 dB compared GS) and virtually vanishes for SMD, which emphasizes its applicability to both BMD and SMD receiver architectures.
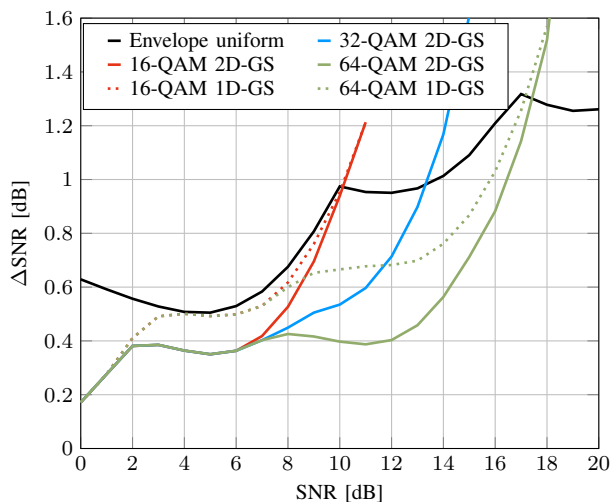

Fig. 3. BMD gap to capacity in dB for 2D-GS.

In Fig. 3, the gap to capacity for 1D-GS $\{16, 64\}$-ary 2D-NUCs and 2D-GS $\{16, 32, 64\}$-ary constellations are shown. The benefits of the additional degrees of freedom are clearly visible.

Summarizing the above results, it becomes evident that both approaches are able to improve the spectral efficiency (SE) of a communication system compared to uniform, equidistant signaling. PS is clearly advantageous for the considered constellation sizes for both BMD and SMD. Hence, the statement of [5], saying that "any gain in capacity which can be found via probabilistic shaping can also be achieved or exceeded

solely through geometric shaping" should be considered with appropriate caution, as it implicitly assumes a much larger constellation size for GS. We illustrate this with two examples for SMD.

Example 1. In [4], the authors provide a signal set construction, where the constellation points are chosen as the centroids of equiprobable quantiles of the Gaussian distribution and show that it is capacity-achieving for $M \to \infty$. An equidistant 8-ASK constellation with optimized distribution using the procedure of Sect. III-B for 10 dB yields $R_{SMD}(P_X^*, 10\,dB) = 1.726\,bpcu$. To achieve the same rate, a number of $M = 50$ constellation points have to be used for their GS approach.

Example 2. In [24], the author describes a practical scheme to construct capacity-approaching APSK constellations consisting of n rings with n constellation points, each. We consider the same case as in Example 1. The PS rate gap, i.e., $C(10\,dB) - R_{SMD}(P_X^*, 10\,dB)$, equals 0.0037 bits per real dimension. According to [24, Fig. 2b], this requires an APSK constellation with much more than $35^2 = 1225$ points and additional two-dimensional demapping.

Similar observations can be found in [25], where the authors investigate the impact of constellation cardinality on the effect of approaching the AWGN channel capacity. They show that the convergence speed of methods like [4] is only $\mathcal{O}(1/M^2)$ (and thus requiring large constellation sizes), whereas the use of Gauss quadratures that involves both geometrical and probabilistic shaping is able to approach capacity exponentially fast in the constellation size.

IV. FEC SIMULATION RESULTS

A. Combining of GS and PS with FEC

We consider soft-decision based binary-input FEC schemes in the following, where the decoder uses real valued log-likelihood ratios (LLRs)

$$L_i = \log\left(\frac{p_{Y|B_i}(y|0)}{p_{Y|B_i}(y|1)}\right) + \log\left(\frac{P_{B_i}(0)}{P_{B_i}(1)}\right), \quad i = 1, \ldots, m. \tag{8}$$

The first term constitutes the channel log-likelihood, whereas the second term represents the priors and evaluates to zero for uniform input distributions.

For GS, the combination with FEC is straightforward and does not require any modifications. However, it remains to note that 2D-GS 2D-NUCs require two-dimensional demapping, so that the LLR calculation has increased complexity.

PAS [2, Sec. IV] employs a *reverse concatenation* of FEC encoding and shaping, while exploiting the symmetry of the optimal input distribution and systematic encoding:

- The symmetric input distribution factors into independent random variables representing the amplitude A and sign S, i.e., $P_X(x) = P_A(|x|)P_S(sign(x))$. While P_A is non-uniform on $\{1, 3, \ldots, 2^m - 1\}$, P_S is uniform on $\{-1, +1\}$.
- The binary representation of the amplitude values is systematically encoded and copied to the codeword, so

that their distribution is preserved. The calculated parity-check bits are approximately uniform and can be used for the sign part.

At the receiver side, the decoder is made aware of the shaping with the help of the priors so that no additional deshaping operation has to be performed. The generation of non-uniform amplitudes from uniformly distributed information bits is accomplished by a distribution matcher (DM) [26].

Apart from closing the gap to the Shannon limit, PAS also enables rate-adaptive transceiver designs [2, Sec. VIII] without changing the modcod. If a 2^m-ASK constellation is used with a rate c code, the SE can be adjusted by the employed distribution P_X and is given by

$$R = \mathrm{H}(X) - (1 - c)m, \tag{9}$$

Hence, rate adaptation can be implemented by adjusting the DM input parameter.

Remark 2. For uniform signaling, equation (9) recovers $R = cm$.

B. Numerical Comparisons with ATSC 3.0

ATSC 3.0 defines 6 constellations (QPSK, {16, 64, 256, 1024, 4096}-NUCs), The smaller ones (16, 64, 256) are 2D-GS 2D-NUCs, whereas the the larger ones (1024, 4096) are 1D-GS 2D-NUCs. The standard also defines low-density parity-check (LDPC) codes with blocklengths 16200 and 64800 bits for code rates from 2/15 to 13/15 [27], giving rise to 46 modcods for the long blocklengths and 29 modcods for the short blocklengths [28].

For each modcod, the standard provides a constellation that has been designed to perform well with the associated code. In Fig. 5, we depict the achievable operating points (AOPs) of all mandatory ATSC 3.0 modcods [8, Table 6.12] involving the {16, 64, 256}-ary 2D-GS 2D-NUCs by considering their gap to capacity. For each modcod, we calculate the required $\mathrm{SNR}_{\mathrm{req}}$ to operate at an SE of $R = \log_2(M) \cdot c$ bits per channel use (bpcu), i.e., $\mathrm{SNR}_{\mathrm{req}} = \mathrm{R}_{\mathrm{BMD}}^{-1}(R)$. For the PAS case, we consider a 256-QAM constellation that is constructed by the Cartesian product of two equidistant 16-ASK constellations and a 5/6 rate code. Following (9), the SE is given as

$$R = \mathrm{H}(X) - \left(1 - \frac{5}{6}\right) \cdot 8 = \mathrm{H}(X) - \frac{4}{3}$$

which can be adjusted by modifying the entropy of P_X. To find the distribution P_X^R that provides an SE of R bpcu, we use the corresponding ν from the family of MB distributions [29, Sec. III-A]. As before, the required SNR is then given as $\mathrm{SNR}_{\mathrm{req}} = \mathrm{R}_{\mathrm{BMD}}^{-1}(P_X^R, R)$. In both cases, the gap to capacity follows as $\Delta\mathrm{SNR} = \mathrm{SNR}_{\mathrm{req}} - \mathrm{C}^{-1}(R)$.

We emphasize that only one single modcod is necessary for PAS to operate within the targeted SE range of 1.0 bpcu to 5.33 bpcu within 0.06 dB.

In the following, we also compare the coded performance of a selection of modcods which are summarized in Table I. This is of interest to evaluate whether the calculated asymptotic
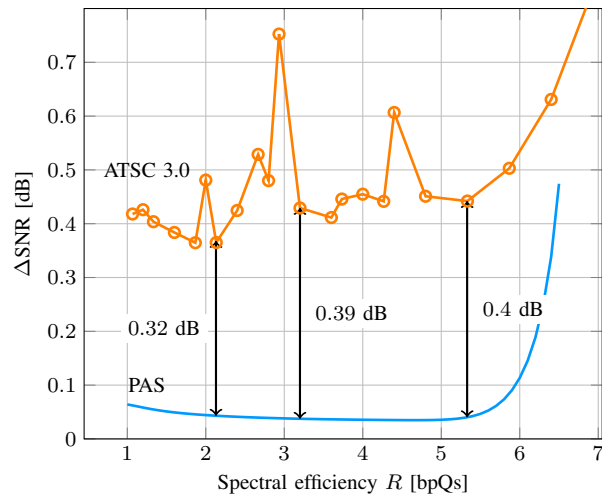

Fig. 5. SNR gap to capacity for ATSC 3.0 AOPs comprising 2D-GS {16, 64, 256} 2D-NUCs and allowed code rates compared to a single PAS modcod of 256-QAM and a 5/6 code.

gains of Fig. 5 derived from information theoretic quantities also translate into practice.

The employed rate 8/15 and 10/15 LDPC codes for the ATSC 3.0 constellations are irregular repeat accumulate (IRA) codes with blocklength 64 800. For each constellation, a different interleaving and bit-mapping is employed according to the standard [8, Table 6.8]. PAS is operated with one single off-the-shelf 5/6 IRA LDPC code from the DVB-S2 standard of the same blocklength with an optimized bit-mapper of [2, Sec. VII-B]. In both cases, 50 belief propagation (BP) iterations with full sum-product update rule at the check-nodes have been performed.

TABLE I
SUMMARY OF THE CONSIDERED MODCODS FOR SEs OF 2.13, 3.2 AND 5.33 bpcu.

SE [bpcu]	Modcod	$R_{\mathrm{BMD}}^{-1}(P_X, R)$ [dB]	Gap [dB]
2.13	PAS 256-QAM, 5/6	5.34	0.043
	ATSC 16-QAM, 8/15	5.66	0.37
3.20	PAS 256-QAM, 5/6	9.17	0.038
	ATSC 64-QAM, 8/15	9.56	0.43
5.33	PAS 256-QAM, 5/6	15.99	0.040
	ATSC 256-QAM, 10/15	16.38	0.44

Looking at Fig. 4, we observe that the predicted performance gains can also be observed in the coded results. For SEs of 3.2 bpcu and 5.33 bpcu, the gains in coded performance even exceed the predicted ones (0.59 dB vs. 0.39 dB and 0.54 dB vs. 0.4 dB). Only for the lowest SE, the gain is slightly smaller than expected (0.31 dB vs. 0.32 dB).

V. CONCLUSION

This work presented a comprehensive comparison of PS and GS for the AWGN channel. We reviewed the underlying optimization problems and explained their mathematical properties. For the non-convex problem of GS, a DE approach was
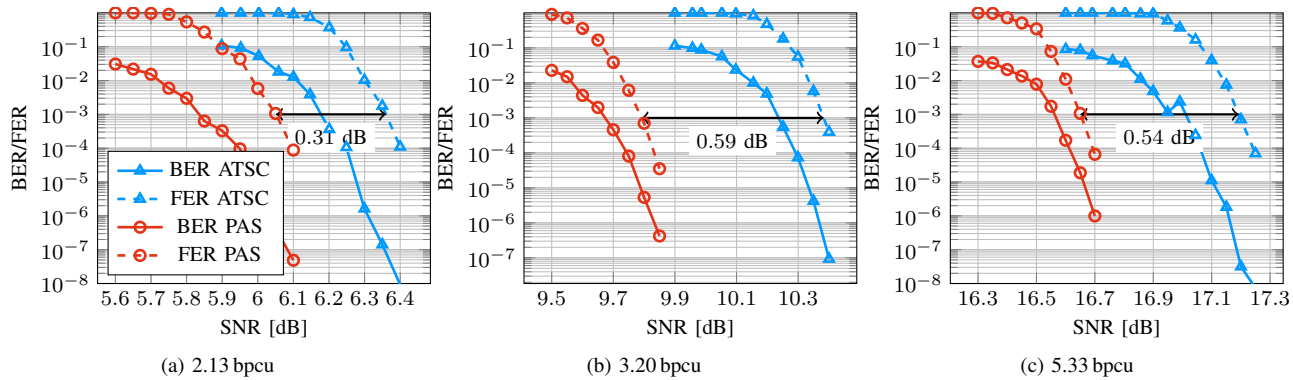
Fig. 4. Comparison of the coded performance of geometrically shaped ATSC 3.0 modcods with one single PAS scheme.

developed. The following achievable rate analysis shows that probabilistic shaping is able to close both the shaping and BMD gap to approach AWGN capacity, whereas a 0.4 dB gap exits for GS. Eventually, we compared the coded performance of different ATSC 3.0 GS modcods to an equivalent setup with only one PS modcod operated via PAS. The predicted gains of the achievable rate analysis can also be observed in the coded scenario. This renders PAS to become a viable candidate for rate-adaptive communication at the Shannon limit for future communication standards.

Acknowledgement

References

[1] G. Forney, R. Gallager, G. Lang, F. Longstaff, and S. Qureshi, "Efficient Modulation for Band-Limited Channels," *IEEE J. Sel. Areas Commun.*, vol. 2, no. 5, pp. 632–647, Sep. 1984.

[2] G. Böcherer, F. Steiner, and P. Schulte, "Bandwidth Efficient and Rate-Matched Low-Density Parity-Check Coded Modulation," *IEEE Trans. Commun.*, vol. 63, no. 12, pp. 4651–4665, Dec. 2015.

[3] M. Valenti and X. Xiang, "Constellation Shaping for Bit-Interleaved LDPC Coded APSK," *IEEE Trans. Commun.*, vol. 60, no. 10, pp. 2960–2970, Oct. 2012.

[4] F.-W. Sun and H. C. A. van Tilborg, "Approaching capacity by equiprobable signaling on the Gaussian channel," *IEEE Trans. Inf. Theory*, vol. 39, no. 5, pp. 1714–1716, Sep. 1993.

[5] M. F. Barsoum, C. Jones, and M. Fitz, "Constellation Design via Capacity Maximization," in *Proc. IEEE Int. Symp. Inf. Theory (ISIT)*, Jun. 2007, pp. 1821–1825.

[6] "Digital Video Broadcasting (DVB);Next Generation broadcasting system to Handheld,physical layer specification (DVB-NGH)," no. A160, Nov. 2013.

[7] D. Gómez-Barquero, C. Douillard, P. Moss, and V. Mignone, "DVB-NGH: The Next Generation of Digital Broadcast Services to Handheld Devices," *IEEE Trans. Broadcast.*, vol. 60, no. 2, pp. 246–257, Jun. 2014.

[8] "ATSC Proposed Standard: Physical Layer Protocol (A/322)," no. S32-230r56, Jun. 2016.

[9] N. S. Loghin, J. Zöllner, B. Mouhouche, D. Ansorregui, J. Kim, and S. I. Park, "Non-Uniform Constellations for ATSC 3.0," *IEEE Trans. Broadcast.*, vol. 62, no. 1, pp. 197–203, Mar. 2016.

[10] R. Storn and K. Price, "Differential Evolution – A Simple and Efficient Heuristic for Global Optimization over Continuous Spaces," *Journal of Global Optimization*, vol. 11, no. 4, pp. 341–359, Dec. 1997.

[11] A. Bennatan and D. Burshtein, "Design and analysis of nonbinary LDPC codes for arbitrary discrete-memoryless channels," *IEEE Trans. Inf. Theory*, vol. 52, no. 2, pp. 549–583, Feb. 2006.

[12] E. Zehavi, "8-PSK trellis codes for a Rayleigh channel," *IEEE Trans. Commun.*, vol. 40, no. 5, pp. 873–884, May 1992.

[13] G. Caire, G. Taricco, and E. Biglieri, "Bit-interleaved coded modulation," *IEEE Trans. Inf. Theory*, vol. 44, no. 3, pp. 927–946, May 1998.

[14] A. Martinez, A. Guillen i Fabregas, G. Caire, and F. Willems, "Bit-Interleaved Coded Modulation Revisited: A Mismatched Decoding Perspective," *IEEE Trans. Inf. Theory*, vol. 55, no. 6, pp. 2756–2765, Jun. 2009.

[15] G. Böcherer, "Achievable rates for shaped bit-metric decoding," *arXiv preprint 1410.8075v6*, 2016.

[16] F. Gray, "Pulse code communication," U. S. Patent 2 632 058, 1953.

[17] J. Zoellner and N. Loghin, "Optimization of high-order non-uniform QAM constellations," in *Proc. IEEE Int. Symp. Broadband Multim. Syst. Broadc. (BMSB)*, Jun. 2013, pp. 1–6.

[18] F. Kayhan and G. Montorsi, "Constellation design for transmission over nonlinear satellite channels," in *Proc. IEEE Global Telecommun. Conf. (GLOBECOM)*, Dec. 2012, pp. 3401–3406.

[19] R. G. Gallager, *Information Theory and Reliable Communication*. John Wiley & Sons, Inc., 1968.

[20] R. E. Blahut, "Computation of channel capacity and rate-distortion functions," *IEEE Trans. Inf. Theory*, vol. 18, no. 4, pp. 460–473, 1972.

[21] J. Huang and S. P. Meyn, "Characterization and computation of optimal distributions for channel coding," *IEEE Trans. Inf. Theory*, vol. 51, no. 7, pp. 2336–2351, Jul. 2005.

[22] F. Kschischang and S. Pasupathy, "Optimal nonuniform signaling for Gaussian channels," *IEEE Trans. Inf. Theory*, vol. 39, no. 3, pp. 913–929, May 1993.

[23] Collection of Optimized 1D-GS and 2D-GS NUCs. [Online]. Available: http://experimental-it.org/research/scc2017/

[24] H. Méric, "Approaching the Gaussian Channel Capacity With APSK Constellations," *IEEE Commun. Lett.*, vol. 19, no. 7, pp. 1125–1128, Jul. 2015.

[25] Y. Wu and S. Verdú, "The impact of constellation cardinality on Gaussian channel capacity," in *Proc. Allerton Conf. Commun., Contr., Comput.*, Sep. 2010, pp. 620–628.

[26] P. Schulte and G. Böcherer, "Constant Composition Distribution Matching," *IEEE Trans. Inf. Theory*, vol. 62, no. 1, pp. 430–434, Jan. 2016.

[27] K. J. Kim, S. Myung, S. I. Park, J. Y. Lee, M. Kan, Y. Shinohara, J. W. Shin, and J. Kim, "Low-Density Parity-Check Codes for ATSC 3.0," *IEEE Trans. Broadcast.*, vol. 62, no. 1, pp. 189–196, Mar. 2016.

[28] L. Michael and D. Gómez-Barquero, "Bit-Interleaved Coded Modulation (BICM) for ATSC 3.0," *IEEE Trans. Broadcast.*, vol. 62, no. 1, pp. 181–188, Mar. 2016.

[29] F. Steiner and P. Schulte, "Design of robust, protograph based LDPC codes for Rate-Adaptation via probabilistic shaping," in *Proc. Int. Symp. Turbo Codes and Iterative Inf. Process. (ISTC)*, Brest, France, Sep. 2016.